

## Articles

# Solubility and Partial Molar Volumes of Naphthalene, Phenanthrene, Benzoic Acid, and 2-Methoxynaphthalene in Supercritical Carbon Dioxide

Z. Sermin Gönenç,<sup>†</sup> Uğur Akman,<sup>†</sup> and Aydın K. Sunol\*

Department of Chemical Engineering, University of South Florida, Tampa, Florida 33620

The effect of temperature, pressure, and supercritical fluid density on the retention and solubility in the mobile phase of solutes in supercritical fluid chromatography was investigated. New retention data for naphthalene, phenanthrene, benzoic acid, and 2-methoxynaphthalene were obtained as a function of pressure at different temperatures. Most of the data were taken near the critical region of the fluid phase where the anomalies such as enhanced solubility/selectivity and retrograde behavior are expected. These data were then used to compare two different approaches for modeling the pressure dependence of solute retention on the column. In these approaches, mobile-phase partial molar volumes of the solutes were determined either from bulk solubility data or from infinite-dilution fugacity coefficients. In both approaches, an integrated expression for the change of retention with pressure was utilized to explicitly reveal the nature of interactions between the stationary phase and the solute. The approach that utilizes the infinite-dilution fugacity coefficient predicts the pressure dependence of solute retention more accurately, especially for solutes that are substantially soluble in the mobile phase near the critical point of the mobile phase. Relationships between the pressure and temperature dependence of the solute solubility in the mobile phase and the retention of solutes on the column were also investigated.

### Introduction

Supercritical fluid chromatography (SFC) is a technique that continues to receive considerable attention for chemical analysis and thermophysical property estimation. Given the existing difficulties in measuring thermophysical properties under supercritical conditions, the SFC-based approach deserves serious consideration, in part due to the ability to accumulate considerable data in a minimal amount of time. The theoretical foundation of this method was developed by Giddings and co-workers and Kobayashi and co-workers in the late 1960s (Kobayashi and Kragas, 1985) in high-pressure chromatography. If the interaction between the supercritical fluid (mobile phase) and the stationary phase is assumed to be negligible, then the retention of a solute depends on its sorptive behavior in the stationary phase, as well as its solubility in the supercritical fluid. Understanding of the retention mechanism is quite important since many of the thermophysical properties are related to the retention volume in SFC.

The effects of temperature, pressure, mobile-phase density, and stationary phase on the behavior of solute retention in SFC have been the subject of recent experimental and theoretical research by several groups (Van Wasen and Schneider, 1980; Yonker and co-workers, 1988; Bartle and co-workers, 1990a,b; Shimm and Johnston, 1989, 1991; Roth, 1990).

Retention data close to the critical point, where anomalies exist, are very limited, resulting in rather poor understanding of the behavior in the region. Therefore, several solutes were used to study the pressure dependence

of the capacity ratio, at different temperatures, particularly near the critical point of the mobile phase. A thermodynamic framework derived through an integrated expression for change of retention with pressure is used, along with infinite-dilution fugacity coefficients, to model the observed retention behavior.

### Experimental Section

The experiments were performed using a Lee Scientific (Salt Lake City, UT) Series 600 supercritical fluid chromatograph. The chromatograph was fitted with a 5 m long, 100  $\mu\text{m}$  i.d. capillary column coated with poly(dimethylsiloxane) of 0.25  $\mu\text{L}$  film thickness. Detection was accomplished with a flame ionization detector. The column temperature and mobile-phase pressure were controlled to an accuracy of  $\pm 0.1$  K and  $\pm 0.01$  MPa, respectively. Retention times were measured using the computer system of the chromatograph within an accuracy of 0.02 s. SFC grade carbon dioxide (supplied by Matheson Gas Products, East Rutherford, NJ) was used as the carrier fluid. The samples (dissolved in pentane) were introduced into the column by means of an automatic injection system. The samples were diluted in pentane until the effect of concentration on retention was negligible, e.i., the samples were assumed to be at infinite dilution in pentane. Methane (supplied by Tampa Oxygen, Tampa, FL) was used to determine the retention time of a compound which is sorbed negligibly in the column stationary phase. Retention data were taken for naphthalene and phenanthrene at various pressures and at isothermal conditions. Naphthalene and HPLC grade pentane were supplied by Fischer Scientific Co. (Pittsburgh, PA), and high-purity phenanthrene, benzoic acid, and 2-methoxynaphthalene were supplied by Aldrich Chemicals (Milwaukee, WI). Ad-

\* To whom correspondence should be addressed.

<sup>†</sup> Department of Chemical Engineering, Boğaziçi University, 80815 Bebek, Istanbul, Turkey.

**Table 1. Pressure, Density, and Capacity Factor data for 2-Methoxynaphthalene**

<i>P</i> /MPa	$\rho_{\text{CO}_2}$ /(g·cm <sup>-3</sup> )	ln <i>k</i>	<i>P</i> /MPa	$\rho_{\text{CO}_2}$ /(g·cm <sup>-3</sup> )	ln <i>k</i>
<i>T</i> = 313 K					
8.11	0.299	1.82	9.42	0.572	-0.26
8.61	0.384	1.15	9.63	0.550	-0.69
8.82	0.438	0.86	9.83	0.614	-0.99
9.12	0.521	0.34	9.93	0.622	-1.24
<i>T</i> = 323 K					
8.11	0.230	2.11	10.13	0.402	0.23
8.61	0.263	1.70	10.64	0.461	-0.34
9.11	0.302	1.25	11.15	0.515	-0.91
9.63	0.348	0.74			

**Table 2. Pressure, Density, and Capacity Factor Data for Naphthalene**

<i>P</i> /MPa	$\rho_{\text{CO}_2}$ /(g·cm <sup>-3</sup> )	$\rho_{\text{SFC}}$ /(g·cm <sup>-3</sup> )	ln <i>k</i>
<i>T</i> = 413 K			
6.08	0.153	0.157	2.41
7.60	0.247	0.247	1.50
7.70	0.256	0.256	1.52
8.11	0.299	0.301	0.97
8.61	0.384	0.408	0.37
8.61	0.384	0.408	0.34
9.12	0.521	0.552	-0.28
9.12	0.521	0.552	-0.26
9.12	0.521	0.552	-0.26
9.32	0.557	0.580	-0.54
9.42	0.572	0.591	-0.67
9.52	0.584	0.601	-0.90
9.63	0.595	0.610	-0.12
<i>T</i> = 318 K			
6.08	0.143	0.149	2.36
7.60	0.220	0.222	1.52
7.60	0.220	0.222	1.50
7.70	0.227	0.228	1.49
8.11	0.256	0.257	1.17
8.11	0.256	0.257	1.16
8.11	0.256	0.257	1.17
8.11	0.256	0.257	1.06
8.61	0.300	0.303	0.66
9.12	0.359	0.370	0.17
9.12	0.359	0.370	0.19
9.63	0.438	0.468	-0.38
9.63	0.438	0.468	-0.37
10.13	0.516	0.553	-0.97
10.13	0.516	0.553	-1.00
<i>T</i> = 323 K			
6.08	0.136	0.141	2.22
7.6	0.202	0.205	1.52
7.6	0.202	0.205	1.49
8.11	0.230	0.232	1.08
8.11	0.230	0.232	1.09
8.11	0.230	0.232	1.09
8.11	0.230	0.232	1.07
8.61	0.263	0.265	0.79
8.61	0.263	0.265	0.77
9.12	0.302	0.304	0.39
9.12	0.302	0.304	0.40
9.12	0.302	0.304	0.40
9.12	0.302	0.304	0.50
9.12	0.302	0.304	0.50
9.63	0.348	0.354	0.02
9.63	0.348	0.354	-0.02
10.13	0.402	0.418	-0.45
10.64	0.461	0.49	-1.00
10.64	0.461	0.49	-0.99

ditional details of the experiments can be found in a previous publication (Gonenc and Sunol, 1992). The measured capacity factors are shown in Table 1–4.

### Theory and Method

As shown in Figure 1, in order to calculate the partial molar volume of the solute in the stationary phase,  $V_s^\infty$ ,

**Table 3. Pressure, Density, and Capacity Factor Data for Phenanthrene**

<i>P</i> /MPa	$\rho_{\text{CO}_2}$ /(g·cm <sup>-3</sup> )	ln <i>k</i>	<i>P</i> /MPa	$\rho_{\text{CO}_2}$ /(g·cm <sup>-3</sup> )	ln <i>k</i>
<i>T</i> = 313 K					
9.32	0.557	0.87	10.34	0.649	-0.90
9.42	0.572	0.87	10.54	0.660	-1.09
9.52	0.584	0.43	10.64	0.665	-1.25
9.63	0.595	0.23	10.64	0.665	-1.23
9.63	0.595	0.21	10.84	0.675	-1.34
9.93	0.622	-0.35	11.15	0.688	-1.60
10.13	0.635	-0.59	11.15	0.688	-1.67
10.13	0.636	-0.64			
<i>T</i> = 323 K					
9.63	0.348	1.77	10.64	0.461	0.58
10.13	0.402	1.21	11.15	0.515	0.00
10.13	0.402	1.20	11.15	0.515	0.11
10.64	0.461	0.56	11.65	0.558	-0.55

**Table 4. Pressure, Density, and Capacity Factor Data for Benzoic Acid**

<i>P</i> /MPa	$\rho_{\text{CO}_2}$ /(g·cm <sup>-3</sup> )	ln <i>k</i>	<i>P</i> /MPa	$\rho_{\text{CO}_2}$ /(g·cm <sup>-3</sup> )	ln <i>k</i>
<i>T</i> = 313 K					
8.41	0.343	1.53	9.42	0.572	0.01
8.61	0.384	1.33	9.63	0.595	-0.44
8.82	0.438	1.02	9.73	0.605	-0.63
9.12	0.521	0.58	9.93	0.623	-0.97
<i>T</i> = 323 K					
8.61	0.263	1.86	10.13	0.402	0.29
9.12	0.302	1.37	10.64	0.461	-0.14
9.63	0.348	0.86	10.64	0.461	-0.28
9.93	0.380	0.48			

the infinite-dilution partial molar volume of the solute in the supercritical mobile phase,  $V_m^\infty$ , has to be evaluated.  $V_m^\infty$  can be calculated either from infinite-dilution supercritical-phase solubility data or from an equation of state where the parameters of the equation of state can be obtained from supercritical solvent/solute solubility data. Although the former is the most desirable method, current lack of extensive infinite-dilution density data limits using this approach.

Two different approaches were used in calculating  $V_m^\infty$ . In approach A,  $V_m^\infty$  is calculated from solubility data available in the literature. Since equilibrium solubilities of some solutes of interest (e.g., naphthalene) are too high to be considered at infinite dilution, the use of the equilibrium mole fractions in calculating  $V_m^\infty$  may not be desirable. In approach B,  $V_m^\infty$  is calculated from the fugacity coefficients at infinite dilution.

Solubility data of the solutes of interest in carbon dioxide were obtained from the literature (McHugh and Paulatis, 1980; Dobbs et al., 1986; Kurnik et al., 1981; Dobbs et al., 1987).

The Peng–Robinson equation of state (PR EOS) (Peng and Robinson, 1976) is often used for representation of the solubility data. For the binary systems of interest, the mixing rule of Panagiotopoulos and Reid (1986), which was developed for asymmetric polar systems, was used.

A van der Waals one-fluid model was used to obtain the parameters of the mixture. The pure-component parameters for the solutes and for the supercritical carbon dioxide were obtained from the usual acentric-factor correlation.

The solid–vapor equilibrium is described with the following thermodynamic relation:

$$y = \frac{P_{\text{sub}}(T)}{P\phi_m(T, P, y)} \exp\left[\frac{V_{\text{sol}}(P - P_{\text{sub}}(T))}{RT}\right] \quad (1)$$

where  $P_{\text{sub}}(T)$  is the temperature-dependent sublimation pressure of the solute,  $\phi_m$  is the supercritical fluid-phase

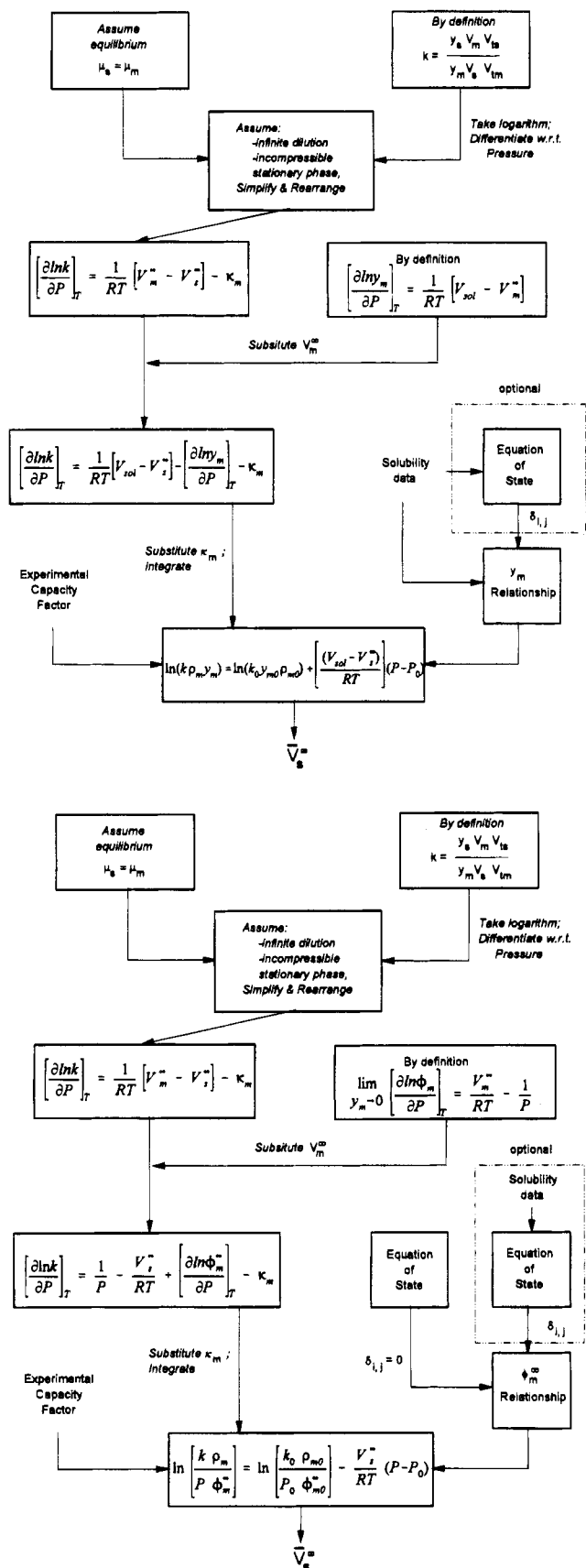


**Figure 1.** (a, top) Procedure for calculation of  $V_s^\infty$  using solubility data. (b, bottom) Procedure for calculation of  $V_s^\infty$  using the infinite-dilution fugacity coefficient.

fugacity coefficient of the solute, and  $V_{sol}$  is the molar volume of the pure solute. The temperature dependence of the sublimation pressures of the solutes in question is given by Jones (1960). Molar volumes of solid solutes of

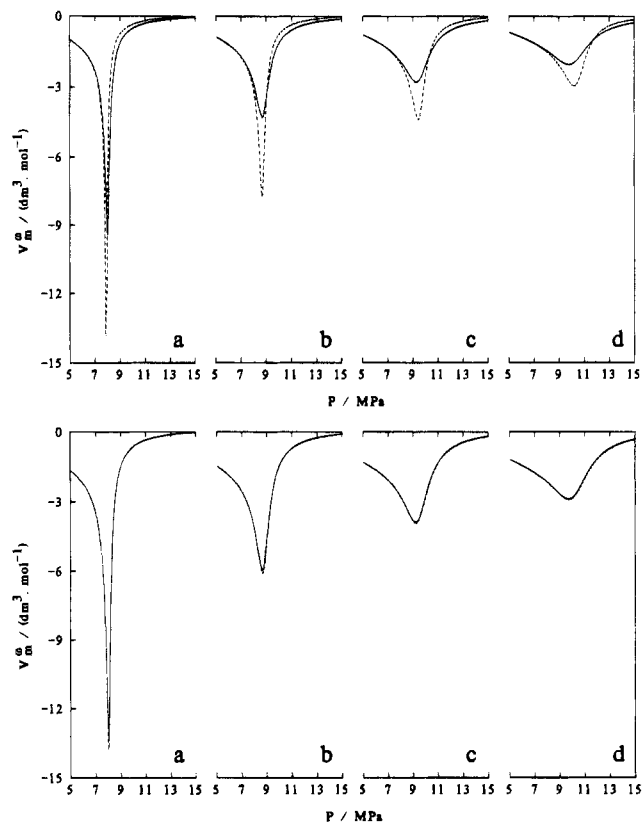


**Figure 2.** (a, top) Infinite-dilution partial molar volume of naphthalene as a function of pressure: (---) calculated from the bulk solubility, (—) calculated from the fugacity coefficient. (a) 308 K, (b) 313 K, (c) 318 K, (d) 323 K. (b, bottom) Infinite-dilution partial molar volume of phenanthrene as a function of pressure: (---) calculated from the bulk solubility, (—) calculated from the fugacity coefficient, (a) 308 K, (b) 313 K, (c) 318 K, (d) 323 K.

**Table 5. Infinite-Dilution Partial Molar Volumes of Solutes in the Stationary Phase**

solute	ap-proach	$V_s^\infty / (\text{dm}^3 \cdot \text{mol}^{-1})$		
		$T = 313 \text{ K}$	$T = 318 \text{ K}^a$	$T = 323 \text{ K}$
naphthalene	A	$-1.80 \pm 0.47$	$-1.17 \pm 0.26$	$-0.72 \pm 0.11$
naphthalene	B	$-1.17 \pm 0.26$	$-0.65 \pm 0.07$	$-0.42 \pm 0.08$
phenanthrene	A	$1.90 \pm 0.25$	ne	$0.16 \pm 0.32$
phenanthrene	B	$2.03 \pm 0.26$	ne	$0.13 \pm 0.33$
benzoic acid	A	$-0.45 \pm 1.15$	ne	$0.45 \pm 0.16$
benzoic acid	B	$-0.54 \pm 1.20$	ne	$-0.52 \pm 0.17$
2-methoxy-naphthalene	B	$-1.46 \pm 1.31$	ne	$-1.04 \pm 0.21$

<sup>a</sup> ne = no experiment.

interest are found in the *International Critical Tables* (1926) as 110.6, 173.9, and 96.5  $\text{cm}^3 \cdot \text{mol}^{-1}$  for naphthalene, phenanthrene, and benzoic acid, respectively. The values of the fugacity coefficient of the solutes ( $\phi_m$ ) were obtained from the PR EOS as described above.

The binary interaction coefficients ( $\delta_{ij}$ ) for naphthalene-, phenanthrene-, and benzoic acid-carbon dioxide systems were obtained through regression of solubility data given in the literature.

The fugacity coefficient  $\phi_m^\infty$  was calculated at infinite-dilution conditions (mole fraction of the solute in the mobile phase  $y_m = 10^{-8}$ ) using PR EOS. It was seen that the value of  $(\partial \phi_m^\infty / \partial P)_m$  did not change significantly when  $y_m$  was decreased below  $10^{-6}$ . Due to the lack of solubility data for the  $\text{CO}_2$ -2-methoxynaphthalene system, the binary interaction coefficient was taken as zero in estimating  $V_s^\infty$  and theoretical values of  $k$ .

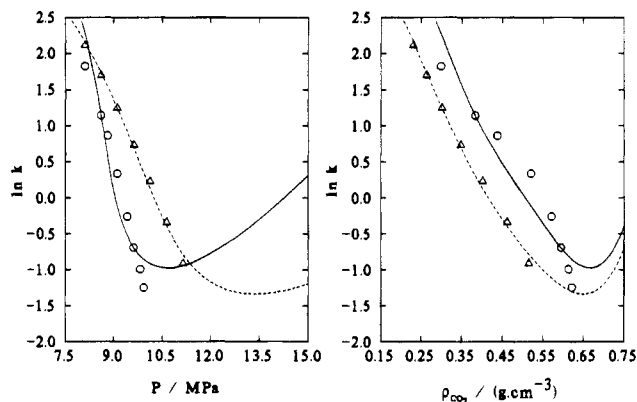


**Figure 3.** Capacity factor of 2-methoxynaphthalene as a function of the pressure and density of carbon dioxide: (---) 323 K, (—) 313 K.

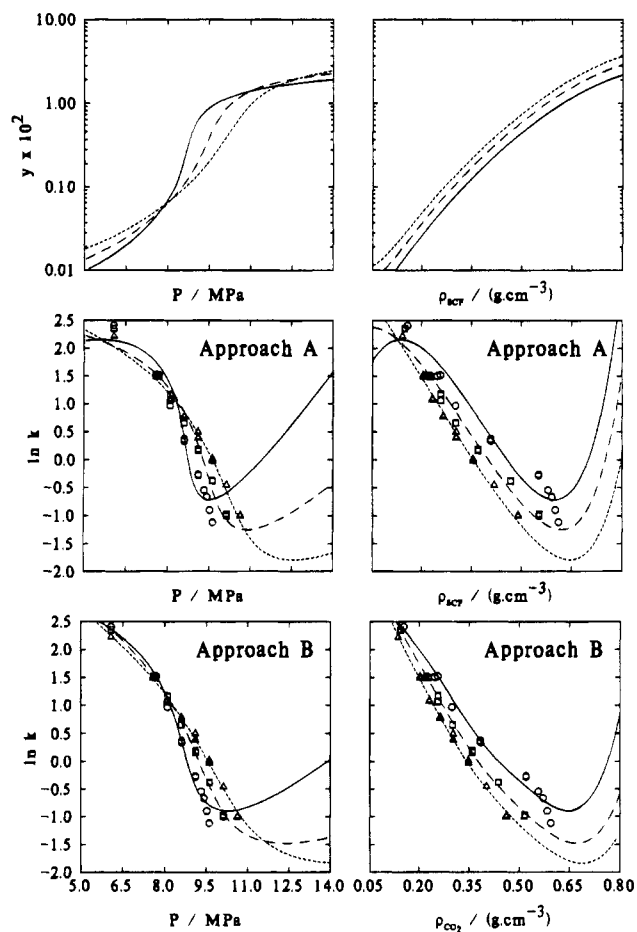


**Figure 4.** Comparison of approaches A and B for the prediction of the capacity factor of naphthalene and the solubility of naphthalene as a function of the pressure and carbon dioxide and supercritical fluid-phase densities: (---) 323 K, (---) 318 K, (—) 313 K.

**Table 6.** Effect of the Interaction Coefficient on Infinite-Dilution Partial Molar Volumes of Solutes in the Stationary Phase for Approaches A and B

solute	T/K	$V_s^\infty / (\text{dm}^3 \cdot \text{mol}^{-1})$					
		approach A			approach B		
		nonzero interaction coefficient	zero interaction coefficient	dev/%	nonzero interaction coefficient	zero interaction coefficient	dev/%
naphthalene	313	$-1.80 \pm 0.46$	$-5.37 \pm 2.41$	198	$-1.17 \pm 0.26$	$-1.61 \pm 0.29$	38
naphthalene	318	$-1.17 \pm 0.20$	$-5.30 \pm 2.07$	352	$-0.65 \pm 0.07$	$-0.95 \pm 0.08$	46
naphthalene	323	$-0.72 \pm 0.11$	$-3.34 \pm 0.14$	361	$-0.42 \pm 0.08$	$-0.66 \pm 0.07$	57
phenanthrene	313	$1.90 \pm 0.25$	$3.79 \pm 0.42$	100	$2.03 \pm 0.26$	$1.25 \pm 0.20$	38
phenanthrene	323	$0.16 \pm 0.33$	$-0.37 \pm 5.34$	5778	$0.13 \pm 0.33$	$-0.74 \pm 0.40$	653

## Results

In order to compare approach A and approach B,  $V_m^\infty$  values for naphthalene, phenanthrene, and benzoic acid were calculated using bulk solubility, as well as infinite-dilution fugacity coefficients. They are shown as a function of pressure for naphthalene (Figure 2a) and phenanthrene (Figure 2b). The values  $V_m^\infty$  calculated using different approaches are quite different for naphthalene, especially near the mobile-phase critical point (Figure 2a). Due to the lower solubility of phenanthrene and benzoic acid in supercritical carbon dioxide, the differences between  $V_m^\infty$  values calculated using approaches A and B are small (Figure 2b).

In approach B, a plot of  $\ln(kQ_m/\phi_m^\infty P)$  versus  $P$  should give a straight line according to Figure 1a. Values of  $V_s^\infty$  are calculated from the slope of such plots (Table 5). Since the bulk solubility of naphthalene in carbon dioxide is about 10 times higher than that of phenanthrene and benzoic acid,  $V_s^\infty$  values determined using bulk solubility and infinite-dilution fugacity coefficients differ for naphthalene more than for the other two solutes (Table 5). For phenanthrene and benzoic acid, the theoretical predictions of  $\ln k$  using  $V_s^\infty$  values calculated through both approaches are similar (Table 5).

Values of  $V_s^\infty$  for 2-methoxynaphthalene, for which no solubility data in carbon dioxide were available, were estimated using approach B (Table 5). Since the binary interaction coefficients could not be calculated in the absence of solubility data, they were assumed to be zero. The behavior is shown in Figure 3.

Although it is theoretically possible to utilize approach A instead, the comparative sensitivity of approach B is far superior. This was shown for naphthalene and phenanthrene for which the results are summarized in Table 6. This was further illustrated in Figure 4. The goodness of the fit of the experimental and theoretical  $k$  values at 323 K may show the negligible effect of the binary interaction coefficient in determining  $V_s^\infty$  for the solute over the specified experimental temperature and pressure ranges.

Figure 4 shows the dependence of solute retention on pressure and mobile-phase density as determined from the chromatographic experiments using the procedure described in Figure 1 and  $V_s^\infty$  values given for naphthalene at 313, 318, and 323 K in Table 5. The equilibrium solubility values are, in general, too high to attain a mole fraction of naphthalene in the SFC at infinite dilution. Discrepancies are observed in the plots drawn using the different approaches; the second approach improved the fit of the  $k$  values to the experimental ones especially at low pressures.

Figures 4 and 5 show the solubilities and retention of the three solutes of concern (naphthalene, phenanthrene, and benzoic acid) as a function of pressure. The figures

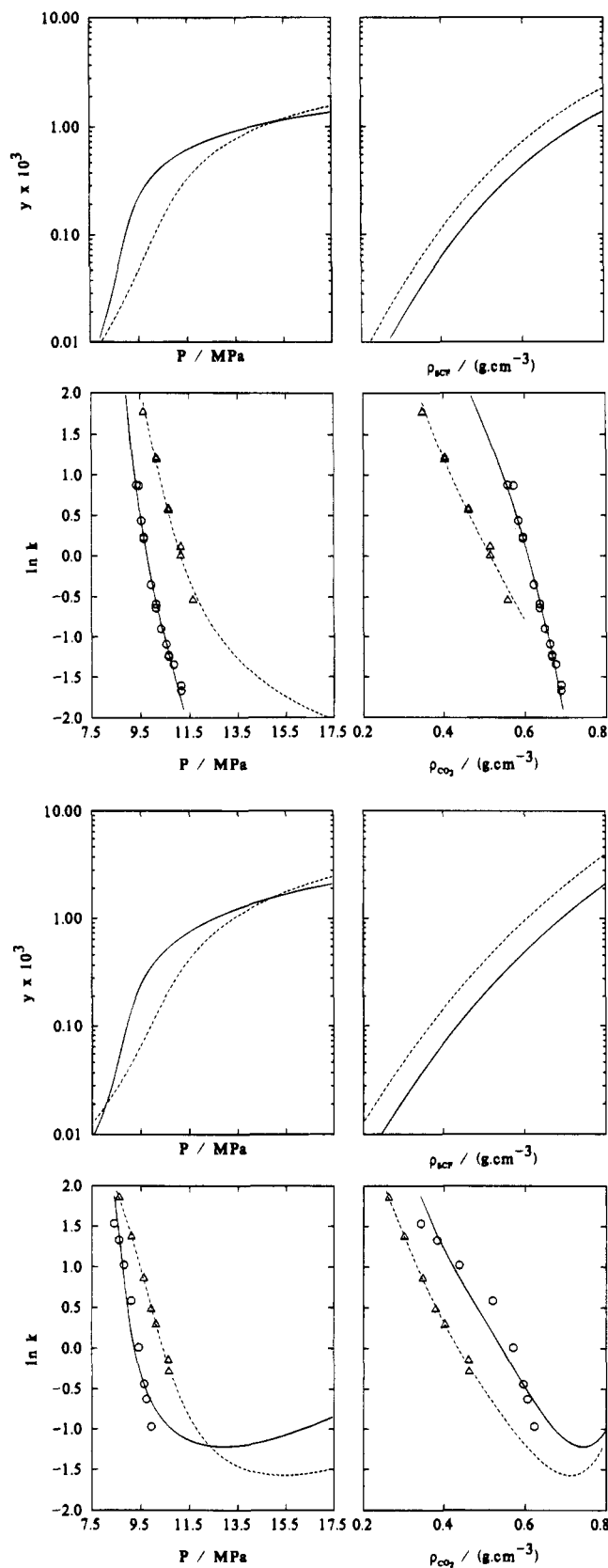


**Figure 5.** (a, top four) Solubility and capacity factor of phenanthrene as a function of pressure and supercritical fluid-phase and carbon dioxide densities: (---) 323 K, (—) 313 K. (b, bottom four) Solubility and capacity factor of benzoic acid as a function of pressure and supercritical fluid-phase and carbon dioxide densities: (---) 323 K, (—) 313 K.

show a direct qualitative relation between the solubility and experimental retention values as a function of temperature. The effect of temperature on the solubility of

naphthalene in carbon dioxide can be discussed for three different pressure regions (Figure 4). In the low-pressure region (less than the critical pressure of the mobile phase), the solubility of naphthalene in carbon dioxide increases as temperature increases. There is a crossover region between the critical pressure of the mobile phase and approximately 10 MPa. In this region, the solubility increases with decreasing temperature for a given pressure. At high pressures ( $P > 10$  MPa), the temperature dependence of the solubility at a fixed pressure is similar to that of the low-pressure region.

This temperature effect in solubility is reflected in the retention of solutes in SFC (Figure 4). At the low-pressure region, solute retention decreases as the temperature increases, which is due to the increase in solubility of the solute in carbon dioxide. At pressures higher than the critical pressure of the mobile phase, the solute retention increases as temperature increases, which is a reflection of the effect of temperature on the solute solubility in the solvent. When the solubility of naphthalene in carbon dioxide is plotted as a function of the mobile-phase density, the previously described crossover behavior is not observed (Figure 4).

At a given mobile-phase density, the solubility of naphthalene in carbon dioxide increases as temperature increases. Figure 4a also shows the effect of the mobile-phase density on the retention of naphthalene. At a given density, the increase in solubility with temperature is reflected on the temperature dependence of retention. As temperature increases, solubility increases, and as a result of this, the retention decreases (Figure 4). This is valid over the entire range of densities for the experimental data.

For other solutes, the experiments were performed only at pressures higher than the critical pressure of the mobile phase. Within the experimental pressure range, the retention of the solutes increased (solubility of the solutes decreased) as temperature increased. Figure 5a shows the experimental and calculated capacity factor of phenanthrene as a function of pressure at 313 and 323 K. The observed behavior of  $\ln k$  with pressure for phenanthrene (as well as for other solutes) is a monotonically decreasing one. For some cases, the predicted behavior may exhibit a minimum. This calculated minimum is due to negative  $V_s^\infty$  values where  $V_m^\infty < V_s^\infty$ , but this was not experimentally observed, and it is a computational artifact of using constant regressed  $V_s^\infty$  values.

Values of  $V_s^\infty$  for benzoic acid at 313 and 323 K are both negative and close to each other (Table 5). Therefore, the predicted values of  $\ln k$  show a similar increase with pressure at both temperatures (Figure 5b). The calculated  $\ln k$  values are closer to the experimentally determined  $\ln k$  values at 323 K than at 313 K.

#### List of Symbols

$k$	capacity ratio
$P$	pressure
$P_{\text{sub}}$	sublimation pressure of the solute
$R$	universal gas constant
$T$	temperature
$V_{\text{sol}}$	molar volume of the solid solute
$V_m^\infty$	infinite-dilution partial molar volume of the solute in the mobile phase
$V_s^\infty$	infinite-dilution partial molar volume of the solute in the stationary phase
$y_m$	mole fraction of the solute in the mobile phase
$y_s$	mole fraction of the solute in the stationary phase

## Greek Symbols

$\delta_{ij}$	binary interaction parameters
$\kappa_m$	isothermal compressibility of the mobile phase
$\mu_m$	chemical potential of the mobile phase
$\mu_s$	chemical potential of the stationary phase
$\rho_m$	molar density of the mobile phase
$\phi_m^\infty$	infinite-dilution fugacity coefficient of the solute in the mobile phase

## Literature Cited

- Bartle, K. D.; Clifford, A. A.; Jafar, B. A. Relationship between Retention of a Solid Solute in a Liquid and Supercritical Fluid Chromatography and its Solubility in the Mobile Phase. *J. Chem. Soc., Faraday Trans.* **1990b**, *86* (5), 855-860.
- Dobbs, J. M.; Wong, J. M.; Johnson, K. P. Nonpolar Cosolvents for Solubility Enhancement in Supercritical Fluid Carbon Dioxide. *J. Chem. Eng. Data* **1986**, *31*, 303-308.
- Dobbs, J. M.; Wong, J. M.; Lahiere, R. J.; Johnston, K. P. Modification of Supercritical Phase Behavior Using Polar Cosolvents. *Ind. Eng. Chem. Res.* **1987**, *26*, 56-65.
- Gonenc, Z. S.; Sunol, A. K. Pressure Dependence of the Partition Coefficient as Measured by Supercritical Fluid Chromatography. *Doga: Turk. J. Chem.* **1992**, *16*, 151-157.
- International Critical Tables*; McGraw-Hill: New York, 1926; Vol. 1.
- Jones, A. H. J. Sublimation Pressure Data for Organic Compounds. *J. Chem. Eng. Data* **1960**, *5*, 196-200.
- Kobayashi, R.; Kragas, T. Adventures in Physico-Chemical Measurements by Gas Chromatography: Past, Present, and Future. *J. Chromatog. Sci.* **1985**, *23*, 11-16.
- Kurnik, R. T.; Holla, S. J.; Reid, R. C. Solubility of Solids in Supercritical Carbon Dioxide and Ethylene. *J. Chem. Eng. Data* **1981**, *26*, 47-51.
- McHugh, M.; Paulatis, M. E. Solid Solubilities of Naphthalene and Biphenyl in Supercritical Carbon Dioxide. *J. Chem. Eng. Data* **1980**, *25*, 326-329.
- Peng, D. Y.; Robinson, D. B. A New Two-Constant Equation of State. *Ind. Eng. Chem. Fundam.* **1976**, *15*, 59-64.
- Roth, M. Thermodynamics of Retention in Supercritical Fluid Chromatography: A Refined Model. *J. Phys. Chem.* **1990**, *94*, 4309-4314.
- Shimm, J.; Johnston, K. P. Adjustable Solute Distribution between Polymers and Supercritical Fluids. *AIChE J.* **1989**, *35* (7), 1097-1106.
- Shimm, J.; Johnston, K. P. Phase Equilibria, Partial Molar Enthalpies and Partial Molar Volumes Determined by Supercritical Fluid Chromatography. *J. Phys. Chem.* **1991**, *95*, 353-360.
- Van Wasen, U.; Swaid, I.; Schneider, G. M. Physicochemical Principles and Application of Supercritical Fluid Chromatography. *Angew. Chem., Int. Ed. Engl.* **1980**, *19*, 575-587.
- Yonker, C. R.; Smith, R. D. Retention in Supercritical Fluid Chromatography: Influence of the Partial Molar Volume of the Solute in the Stationary Phase. *J. Phys. Chem.* **1988**, *92*, 1664-1667.

Received for review September 19, 1994. Revised January 25, 1995. Accepted March 5, 1995.\*

JE940195O

\* Abstract published in *Advance ACS Abstracts*, May 1, 1995.